


## Article

# Effects of Ti6Al4V Surfaces Manufactured through Precision Centrifugal Casting and Modified by Calcium and Phosphorus Ion Implantation on Human Osteoblasts

Fiedler Jörg <sup>1</sup> , Katmer Amet Betül <sup>1</sup>, Michels Heiner <sup>2</sup>, Kappelt Gerhard <sup>3</sup>  
and Brenner Rolf Erwin <sup>1,\*</sup>

<sup>1</sup> Department of Orthopedic Surgery, Division for Biochemistry of Joint and Connective Tissue Diseases, Ulm University, 89081 Ulm, Germany; joerg.fiedler@uni-ulm.de (F.J.); betuel.katmer@uni-ulm.de (K.A.B.)

<sup>2</sup> Access e.V., 52072 Aachen, Germany; h.michels@access-technology.de

<sup>3</sup> Peter Brehm GmbH, 91085 Weisendorf, Germany; gerhard.kappelt@peter-brehm.de

\* Correspondence: rolf.brenner@uni-ulm.de; Tel.: +49-731-500-63281

Received: 30 October 2020; Accepted: 9 December 2020; Published: 16 December 2020



**Abstract:** (1) In order to enable a more widespread use of uncemented titanium-based endoprostheses to replace cobalt-containing cemented endoprostheses for joint replacement, it is essential to achieve optimal osseointegrative properties and develop economic fabrication processes while retaining the highest biomedical quality of titanium materials. One approach is the usage of an optimized form of Ti6Al4V-precision casting for manufacturing. Besides the chemical and physical properties, it is necessary to investigate possible biological influences in order to test whether the new manufacturing process is equivalent to conventional methods. (2) Methods: Primary human osteoblasts were seeded on discs, which were produced by a novel Ti6Al4V centrifugal-casting process in comparison with standard machined discs of the same titanium alloy. In a second step, the surfaces were modified by calcium or phosphorus ion beam implantation. In vitro, we analyzed the effects on proliferation, differentiation, and apoptotic processes. (3) Results: SEM analysis of cells seeded on the surfaces showed no obvious differences between the reference material and the cast material with or without ion implantation. The MTT (3-(4,5-dimethylthiazol-2-yl)-2,5-diphenyltetrazolium bromide) proliferation assay also did not reveal any significant differences. Additionally, the osteogenic differentiation process tested by quantitative polymerase chain reactions (PCR), Alizarin red S assay, and C-terminal collagen type I propeptide (CICP) Elisa was not significantly modified. No signs of induced apoptosis were observed. (4) Conclusions: In this study, we could show that the newly developed process of centrifugal casting generated a material with comparable surface features to standard machined Ti6Al4V material. In terms of biological impact on primary human osteoblasts, no significant differences were recognized. Additional Ca- or P-ion implantation did not improve or impair these characteristics in the dosages applied. These findings indicate that spin casting of Ti6Al4V may represent an interesting alternative to the production of geometrically complex orthopedic implants.

**Keywords:** Ti6Al4V; centrifugal casting; ion implantation; human osteoblast

## 1. Introduction

Nowadays, there is high demand for cost-effective knee joint endoprosthesis in orthopedic arthroplasty. The currently used respective Gold standard material for cemented endoprosthesis, Co28Cr6Mo, however, is in discussion in terms of biocompatibility and longevity because of its cobalt

content. Ti6Al4V is the most frequently used titanium-alloy for uncemented orthopedic endoprosthesis implantation, but fabrication of standard 3-dimensional structures for joint arthroplasty involves cost intensive usage of machining blanks and milling machines to remove projecting titanium parts [1].

Therefore, a cost-effective titanium casting process could achieve improvement in several ways. It could lead to the partial replacement of cobalt-containing implants and avoid the use of bone cement in these cases based on superior features of osseointegration. However, because of the high melting point of titanium and its unfavorable fluidity and reactivity in a molten state, this fabrication procedure is not routinely used so far [2,3].

As described previously, an optimized centrifugal casting process, including casting and cooling conditions, crucible and mold material, and enhanced heat treatment facilitates, was used for the manufacturing of near net-shape titanium-based implants (Figure 1 is an illustration of a centrifugal precision casting device from Michels, Aachen, Germany) [4]. In the applied casting process on the Leicomelt 5 TP casting device, the solid metal alloy is placed in a cold wall crucible. This type of crucible consists of a ring-shaped wall of water-cooled palisades made from copper. A magnetic alternating field is induced by the application of current to an induction coil surrounding the palisade package. This field generates heat in the alloy material due to ohmic losses, eventually melting the solid alloy. Melting and subsequent casting is carried out under an inert gas/vacuum atmosphere. The liquid metal is poured by tilting the crucible through a separation valve between the melting and casting chamber into a heating box containing the casting setup consisting of sprue, melt distributor and ceramic shell mold. The heat box and casting setup are fixed on a rotating table inside the casting chamber. Prior to the pouring of the melt, the casting the table is set into a rotation of up to 400 RPM, creating rotational forces on the liquid metal as it enters the casting setup. Following the applied force, the melt flows into the ceramic shell mold, thus filling it within 1.5 s. The cooled down metal is manually freed from the ceramic shell mold, and the *in vitro* samples are cut by a water jet.

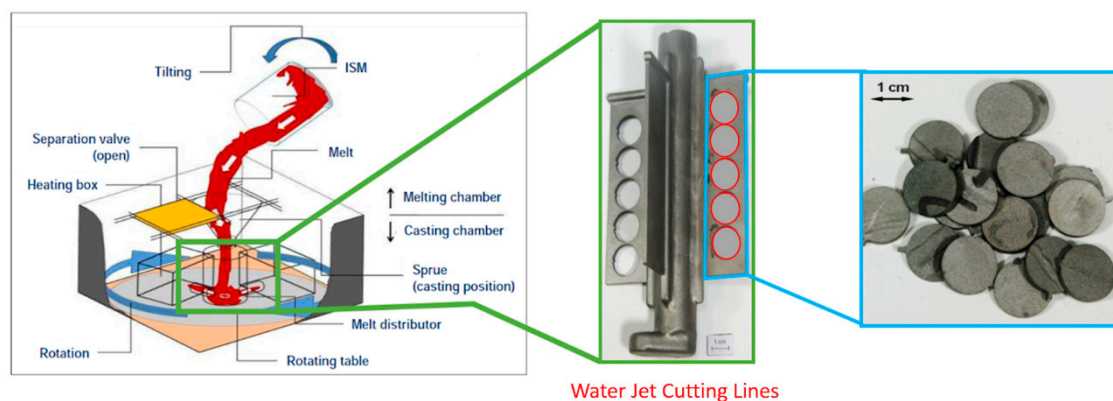


**Figure 1.** Principal centrifugal casting layout (Leicomelt TP5) (left); cast part wax model providing 4 rectangular plates, water jet cutting lines in red (center); water-jet cut of *in vitro* test specimen (right). Discs were 14 mm in diameter and 2 mm in height.

Besides the complex manufacturing process of titanium-based implants, it is necessary to focus on their biological aspects. Stability after uncemented implantation into bone depends on a proper interaction between the material and the cells of the surrounding tissue, especially osteoblasts [5]. While pure titanium or titanium-based alloys like Ti6Al4V are usually regarded as having excellent mechanical and biocompatibility properties, several organic and inorganic surface modifications were used to further enhance osseointegration [6]. With respect to inorganic components, besides surface modification by the addition of hydroxyapatite, complex 3-dimensional structures were generated by plasma treatment in order to deposit calcium or phosphorus ions onto the surfaces [7,8]. Since delamination of hydroxyapatite coatings with negative long-term effects has been reported [8,9],

ion implantation of calcium and phosphorus into the material surface has been tested, encouraging the formation of calcium phosphate precipitates [10,11]

The alloy surface should maintain the cell adhesion, proliferation and differentiation processes of osteoblasts, which are dependent on biochemical, topographical and biomechanical parameters. One example is the increasing response of different cells to materials using nano topography by supporting respective adhesion and proliferation [12,13]. With respect to osseointegration, the material should not decrease the expression of necessary osteogenic differentiation factors like RUNX2 (Runt-related transcription factor 2) or the synthesis of collagen type I, which is essential for extracellular matrix synthesis [14].

The aim of this *in vitro* study was to investigate the possibilities of using machine blanks and milling machines to transfer a medical grade process of knee endoprosthesis production into a more cost-effective, less material consuming optimized centrifugal casting process, without worsening the biological effects on primary human osteoblasts. We used a modified manufacturing technique for the production of near net-shape precision centrifugal castings of Ti6Al4V, representing an alloy widely used for medical treatment. In addition, a calcium and phosphorus ion beam implantation into the implant's surface was tested to see if it modified the biological outcome.

## 2. Materials and Methods

An overview of the experimental setup is given in Figure 2. Besides the used test specimen, the cell biological tests are illustrated.

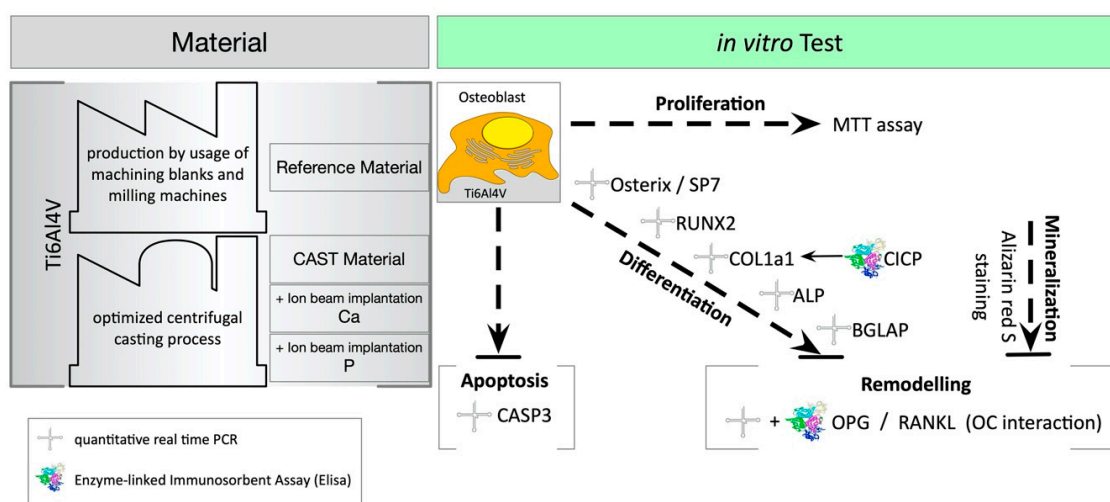


**Figure 2.** Scheme of the materials and methods used for *in vitro* testing. The medical grade alloy Ti6Al4V was processed under standard conditions (reference material; REF) or in the optimized centrifugal casting process (CAST). Some specimens were modified by ion beam insertion of Ca- or P-ions into the surface. Discs of 14 mm in diameter were seeded with human primary osteoblasts and underwent different *in vitro* testing. Cell biologic analysis focused on cell proliferation, osteogenic differentiation, matrix mineralization, remodeling processes, and apoptosis.

MTT: colorimetric assay of cellular metabolic activity by reducing the tetrazolium dye MTT 3-(4,5-dimethylthiazol-2-yl)-2,5-diphenyltetrazolium bromide to its insoluble formazan. Alizarin red S: staining of the calcified matrix that is synthesized by the osteoblasts. Quantitative real time PCR: gene expression analysis of differentiation markers. Osterix/SP7: a transcription factor that is highly conserved among bone-forming cells and responsible for osteogenic differentiation. RUNX2: Runt-related transcription factor 2 associated with osteoblast differentiation. COL1a1: collagen type I alpha 1 as one chain of collagen type I—the major structural protein of bone. C1CP: type I C-terminal collagen propeptide. ALP: tissue non-specific Alkaline phosphatase. BGLAP: osteocalcin, also known

as bone gamma-carboxyglutamic acid-containing protein, is a calcium binding protein. CASP3: caspase-3 plays an important role in cell apoptosis. OPG: osteoprotegerin, a protein produced by osteoblasts to counteract bone resorption by osteoclasts. RANKL: the receptor activator of nuclear factor kappa-B ligand, stimulator of bone resorption. OC: osteoclasts.

### 2.1. Primary Human Osteoblasts

Primary human osteoblasts were isolated from human bone specimens collected from routine joint replacement surgery with the consent of patients and after approval from the local ethics committee of the University of Ulm. Overall, samples from 7 donors were used. Cells were isolated and cultivated under standard conditions as described previously [15].

### 2.2. Test Specimen

For the in vitro testing, discs of the respective materials with a diameter of 14 mm and a height of 2 mm were used. The reference test specimens (REF) consisted of machined, aluminum-oxide-blasted Ti6Al4V and were manufactured by Peter Brehm GmbH (Weisendorf, Germany). The spin-cast discs were manufactured by the optimized centrifugal precision-casting technique, which was developed in cooperation between the independent research facility Access e. V. (Aachen, Germany) and the implant manufacturer, Peter Brehm GmbH (Weisendorf, Germany), as described earlier [6]. Following the casting process, the parts were heat HIPed (hot-isostatic pressed) according to Ti6Al4V standard procedures and parameters (1000 bar at 920 °C for 120 min). During the HIP procedure, by parallel application of temperature and pressure, the porosity in the cast part is effectively reduced, increasing the density of the cast material by significantly decreasing the volume fraction of possibly existing casting defects. The test specimens created by the melting cast procedure (CAST) were cut out of bigger sized plates to maintain the typical surface features generated by the casting process. Finally, the CAST discs were aluminum-oxide-blasted, using the same standard process as for the reference material [6].

Ion beam implantation was used to modify the properties of material surfaces [15]. Ca- or P-atoms were ionized and accelerated in electric fields and thus implanted into the surface of planar Ti6Al4V seals. The implantation was carried out with a conventional low-energy implant DANFYSIK 1050 (Danfsik, Taastrup, Denmark) at the Helmholtz-Zentrum Dresden-Rossendorf (HZDR), as described previously for Cu- and Ag-ions [15]. The surfaces were implanted with an energy of 30 keV and a dose of  $1 \times 10^{-16}$  cm<sup>2</sup> Ca- or P-ions.

### 2.3. SEM Analysis of Cell Adhesion

The surface structure of the discs and cell adhesion were investigated by using scanning electron microscopy Hitachi S-5200 (Hitachi, Tokyo, Japan) at the electron microscopy core facility of the University of Ulm, Germany. Specimens without cells were sputtered with gold-palladium (20 nm) under standard conditions. Specimens with cells were first fixed with 2.5% glutaraldehyde and 1% saccharose in 0.1 M of phosphate buffer before sputtering with gold-palladium.

### 2.4. Molecular Biological Methods

Gene expression analysis was performed with standard methods, as described earlier [16]. Human osteoblasts were seeded at a density of 20,000 cells per disc, which was placed in one well of a 24-well plate and covered with 1 ml of Dulbecco's Modified Eagle Medium (DMEM), 10% fetal calf serum (FCS), 100 µL penicillin/streptomycin solution, and 2 mM L-glutamine (all Biochrome, Berlin, Germany). For differentiation processes, 0.1 µM dexamethasone, 10 mM β-glycerophosphate, and 0.2 mM L-Ascorbic acid (all Sigma-Aldrich, Steinheim, Germany) were added to the medium.

For normalization of the quantitative real-time polymerase chain reaction (PCR) results, a cell sample of osteoblasts before seeding on the titanium surfaces was used in all experiments. The cell culture supernatant was used for Enzyme Linked Immuno Sorbant Assay (Elisa). The cells were lysed by using the RNeasy kit from Qiagen (Qiagen, Hilden, Germany), following company instructions.

Synthesis of cDNA was carried out with the Omniscript kit from Qiagen (Qiagen, Hilden, Germany) in accordance with the given manuals. Gene expression was analyzed using a TaqMan StepOne Plus (Life Technologies, Darmstadt, Germany) and ready-to-use TaqMan probes, which are commercially available from Life Technologies (listed in Table 1). Amplifications were carried out using the TaqMan Fast Advanced Master Mix (Life Technologies, Darmstadt, Germany). Gene expressions were calculated with the  $\Delta\Delta C_t$  method and normalized to HPRT1 as a housekeeping gene [17].

**Table 1.** The TaqMan probes and targets used. Probes were designed and tested for specificity by Life Technologies (Darmstadt, Germany).

Gene	Gene Accession No.	TaqMan Assay ID	Common Name
ALP	NM_000478.5	Hs01029144_m1	Alkaline phosphatase
BGLAP	NM_199173.5	Hs01587814_g1	Bone gamma-carboxyglutamate protein
CASP3	NM_004346.3	Hs00234387_m1	Caspase 3
COL1a1	NM_000088.3	Hs00164004_m1	Collagen type I alpha 1
HPRT1	NM_000194.2	Hs02800695_m1	Hypoxanthin-Phosphoribosyl-Transferase 1
OPG	NM_002546.3	Hs00900358_m1	Osteoprotegerin
RUNX2	NM_001015051.3	Hs00231692_m1	Runt-related transcription factor 2
TNF	NM_000594.3	Hs01113624_g1	Tumor necrosis factor
RANKL	NM_003701.3	Hs00243522_m1	Receptor activator of nuclear factor kappa-B ligand
SP7	NM_001173467.2	HS001866874_s1	Transcription factor Sp7, Osterix

Gene and Gene Accession No. from GeneBank, NIH, TaqMan Assay ID given identification No from Life Technologies.

## 2.5. Elisa

In order to analyze protein secretion, a human Osteoprotegerin Instant ELISA (affymetrix, San Diego, CA, USA) and a MicroVue® Bone CICP EIA Elisa (Quidel, San Diego, CA, USA) were used according to the manufacturers' instructions. The Elisases were analyzed using a Tecan Infinite M200 Pro (Tecan, Männedorf, Switzerland) for readout and the software iControl™ V. 1.2 or Magellan™ V. 7.2 for, all from Tecan, Männedorf, Switzerland).

## 2.6. MTT Assay

Cell proliferation was tested according to DIN ISO 10993-5 by using tetrazolium salt MTT (3-(4,5Dimethylthiazol-2-yl)-2,5-diphenyltetrazoliumbromid) as described elsewhere. Staining was conducted 24 h, 3 days, and 7 days after cell seeding on the specimen, which was cultivated under standard conditions [15]. At the indicated time points, the discs were placed into fresh wells of a 24-well plate in order to only include cells seeded on the titanium surface. The wells were filled with 1 mL MTT solution and incubated for 3 h. Then, the MTT solution was replaced by 200 µL of a 0.04 M HCl/Isopropanol mixture. The discs were reversed using forceps and sonicated for 3 min. The staining was analyzed with a Tecan Infinite M200 Pro (570 nm/650 nm), as described above (Section 2.5).

## 2.7. Alizarin Red S Staining

To prove the matrix calcification of the seeded specimens, Alizarin red S staining was performed. Therefore, 20,000 cells per disc were cultivated for 14 days in basal medium with the additional supplements as indicated above (Section 2.4). Then, the discs were placed into a new well and washed three times with 1 mL phosphate buffered saline (Biochrome, Berlin, Germany). Subsequently, 1 mL of 70% ethanol was added and incubated for 1 h. Thereafter, 1 mL of a 40 nM Alizarin staining solution was added and incubated on a horizontal shaker for 10 min. After several washing steps with pure water, an incubation for 15 min with 10% cetylpyrimidinchloride was performed. 100 µL was used to analyze the concentration of Alizarin red S using a Tecan Infinite M200 Pro plate reader (absorbance 652 nm), as described above (Section 2.5).



## 2.8. Statistical Testing

Statistical analysis was carried out using GraphPad Prism version 8.4 for Macintosh (GraphPad Software, La Jolla, San Diego, CA, USA, ([www.graphpad.com](http://www.graphpad.com))). Depending on the experimental setup, a one-way-Analysis of Variance (ANOVA) or two-way-ANNOVA was used. A Tukey post hoc test was performed for one-factorial analysis of variance; a Bonferroni post hoc test was used for two-factorial analysis. The level of significance was set to  $p < 0.05$ . The data are presented by a Scatter-dot plot with Median and interquartile range.

## 3. Results

Before cutting the test specimen, each plate was checked for the existence of Alpha Case, a critical surface feature, which can develop during the cooling phase of the casting process due to the presence of oxygen. While thin layers can be removed by etching, generally avoiding the formation of Alpha Case during the casting process is the preferred solution with respect to cost-effective part production. Figure 3 shows typical analyses of cast part samples before (Figure 3A,C) and after (Figure 3B,D) optimization of the employed centrifugal casting process, indicating that Alpha Case formation could be completely prevented in the test samples used for further analyses (Figure 3B,D).

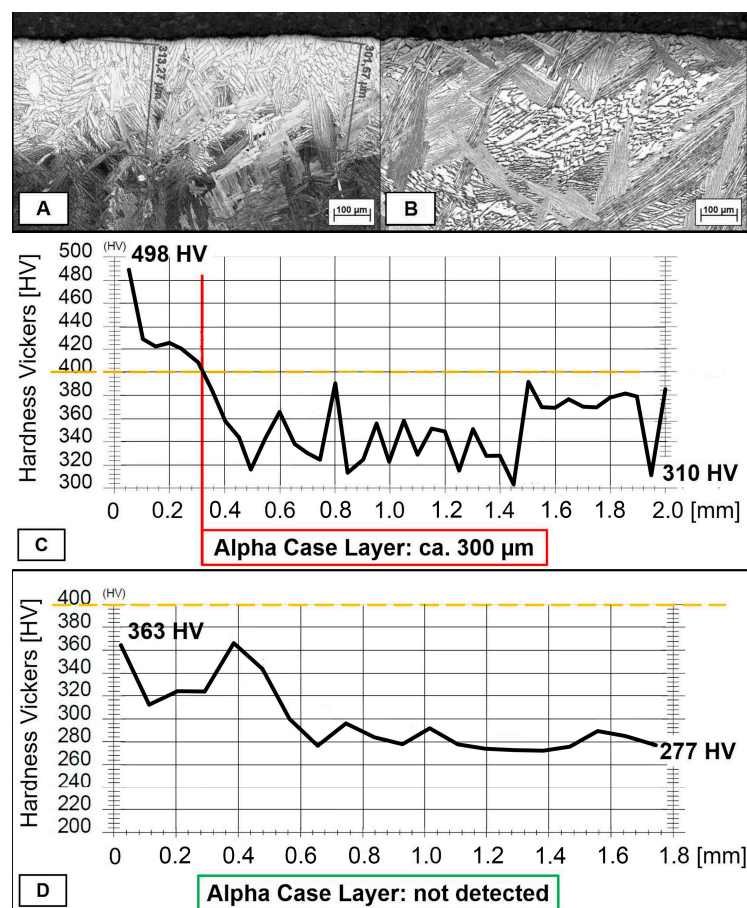


**Figure 3.** Microstructure analysis (Light Microscopy 100× magnification; Micro-Hardness) (A,C) Microstructure before process optimization, thickness of Alpha Case Layer critical ( $>15 \mu\text{m}$ ); (B) and (D) Microstructure after process optimization, no Alpha Case detectable (Hardness Vickers, Load: HV0.10, Obj. 50×).

The chemical composition of the test specimen was checked by Inductively Coupled Plasma-Optical Emission Spectrometry (ICP-OES) analysis according to DIN 51008-2/DIN 51009. ICP-OES is

an elemental analysis method to determine sample compositions on trace-level. Samples are water dissolved and conducted through a nebulizer into a spray chamber. The resulting aerosol is lead through an argonized plasma chamber operating at around 6000 to 7000 K. The aerosol takes up thermal energy and atomization, and ionization takes place. Electrons reach a higher state for a short amount of time and eventually drop back to ground level energy. While dropping back, energy is liberated as light waves (photons). For each element, the wavelength of the emitted light is characteristic and used to identify the elements present in the sample. Information regarding the content of an element is provided by the measured intensity of the detected wave lengths. Based on the machine calibration, these values are used to calculate the concentration of elements contained in the sample.

Representative results are shown in Table 2. The element amounts were within the specified boundaries and the results show a typical decrease of Al and an increase of elements such as Cu, Fe and Ti, respectively. This effect commonly occurs when a melting alloy containing Al is used at high temperatures. However, this effect is minimal for the Leicomelt 5 TP device, as shown by the results.

**Table 2.** Element concentration as specified for Ti6Al4V ELI and measured for the alloy material before and after the melting+casting+HIP process chain. Tests were conducted by Elektrowerk Weisweiler GmbH (Eschweiler-Weisweiler, Germany). Results are shown in weight percent (wt.%).

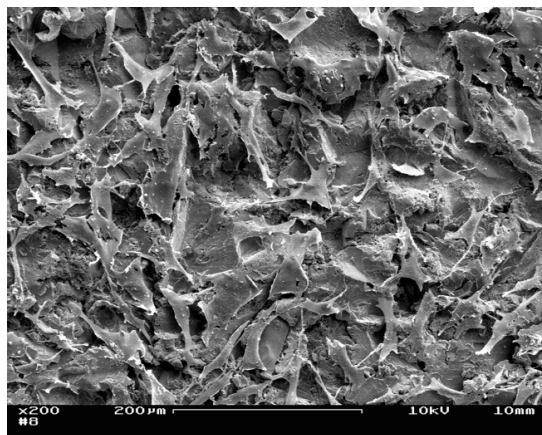
Element	Ti6Al4V ELI Specification	wt.% before Processing	wt.% after Melting, Casting & HIP
C	0.1 (max)	0.011	0.053
V	3.5–4.5	4.53	4.43
Al	5.5–6.75	6.18	6.03
O	0.2 (max)	0.176	0.131
N	0.05 (max)	0.005	0.001
Fe	0.3 (max)	0.215	0.223
H	0.015 (max)	0.005	0.012
Y	-	<0.001	<0.002
Ti	Balance	Balance	Balance

### 3.1. Surface Characteristics and SEM Analysis

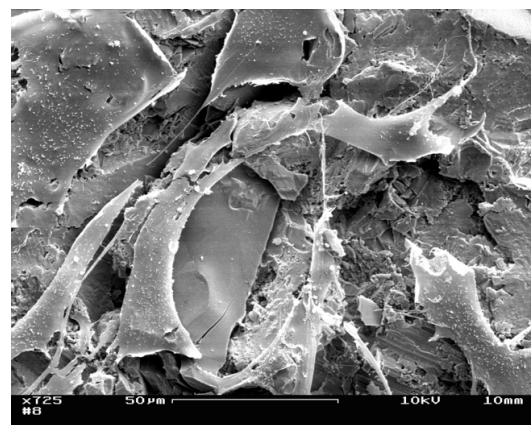
The biocompatibility of medical implants is determined by several factors. Although the reference and cast specimens used in this study were made of the same titanium alloy and had a comparable major chemical composition as mentioned above, effects on the cell adhesion, proliferation, and differentiation of human osteoblasts could be influenced by the respective surface profile. Therefore, surface micro-topography was characterized.

When analyzing the average roughness Ra and Rz by using standard procedures, no significant differences were detected. For the reference surfaces, the mean value of Ra was 5.1  $\mu\text{m}$  (SD 0.44  $\mu\text{m}$ ), while a Rz of 29.78  $\mu\text{m}$  (SD 1.71  $\mu\text{m}$ ) was measured. For the cast samples, the mean value determined for Ra was 4.55  $\mu\text{m}$  (SD 0.14  $\mu\text{m}$ ) and Rz ranged from 28.05  $\mu\text{m}$  (SD 2.18  $\mu\text{m}$ ). In ion implanted surfaces, samples with implanted Ca-ions showed mean values of Ra 4.45  $\mu\text{m}$  (SD 0.43  $\mu\text{m}$ ) and Rz 27.20  $\mu\text{m}$  (2.53  $\mu\text{m}$ ). In cast specimens with implanted P-ions, Ra was measured with 4.86  $\mu\text{m}$  (SD 0.45  $\mu\text{m}$ ), and Rz 29.58  $\mu\text{m}$  (SD 2.07  $\mu\text{m}$ ) was detectable.

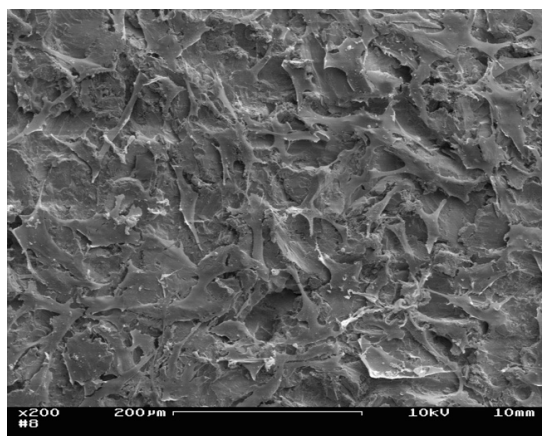
By using scanning electron microscopy, we could further show that the surfaces of both types of specimen were similar and that the seeded human osteoblasts could adhere and cover the surface after several days, as shown in Figure 4. Additionally, no different seeding behavior was observed after the ion beam implantation of calcium or phosphorus ions into the surface. The osteoblasts were comparable in terms of their cellular morphology and size.



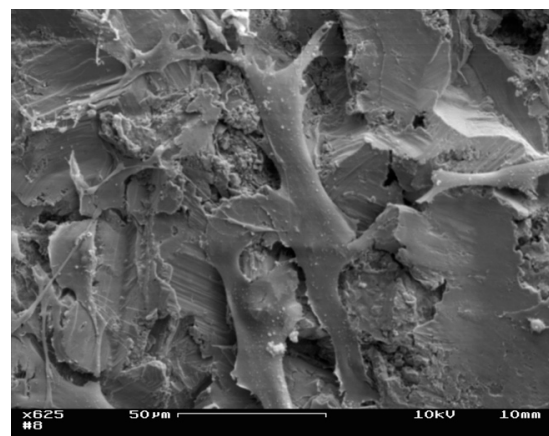
(a)



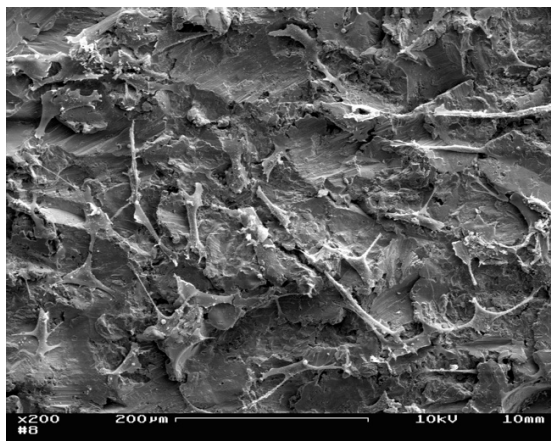
(b)



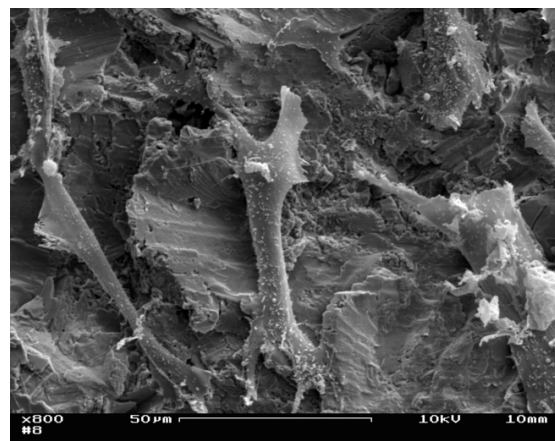
(c)



(d)



(e)



(f)

Figure 4. Cont.



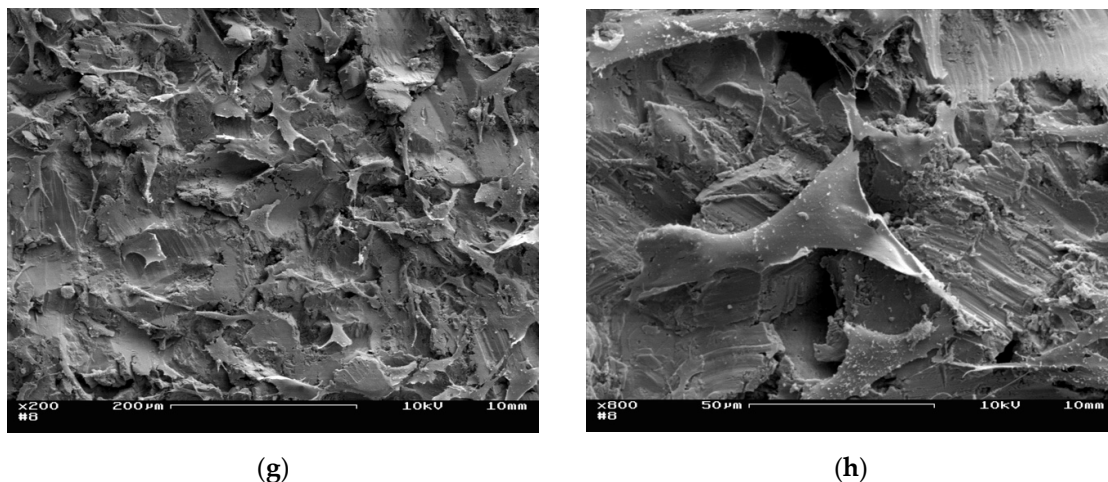


**Figure 4.** SEM images of cell seeded surfaces. On all shown pictures, primary human osteoblasts were cultivated for three days under standard conditions. Reference material (a) 200 k and (b) 725 k (magnification). Cast specimens (c) 200 k and (d) 625 k (magnification). Cast specimens with ion beam implantation of Ca (ion density  $1 \times 10^{-16} \text{ cm}^2$ , energy level 30 keV) ((e) 200 k and (f) 800 k magnification). Cast discs with ion beam implantation of P (ion density  $1 \times 10^{-16} \text{ cm}^2$ , energy level 30 keV) ((g) 200 k and (h) 800 k magnification). Scanning electron microscopy was performed using a Hitachi S-5200 (Tokyo, Japan). Pictures were taken from [18] with permission.

It can be summarized that conspicuous changes in cell morphology could be detected on none of the investigated casting surfaces. Therefore, with regard to cell adhesion and cell spreading, an equivalence between centrifugal casting and the current reference surfaces can be assumed. Additionally, the ion beam implantation of calcium or phosphorus ions did not obviously affect the respective cellular response.

### 3.2. Cell Adhesion and Proliferation

In terms of biocompatibility, the cell adhesion and proliferation/viability measured by MTT-assay can be used as a well-established tool for characterizing cellular interaction with biomaterials. As shown in Figure 5, on all tested surfaces the human osteoblasts could adhere in equal amounts after 24 h. No statistically significant difference was observed between the reference material and the specimen produced by centrifugal casting. In addition, after cultivation for 7 days, no significant difference could be identified. Regarding the time of cultivation, a significant difference between day 1 and day 7 was detectable for the reference (REF) and the cast material (CAST). The ion implantation of P led to a nearly significant increase from day 1 to day 7 (CAST+P;  $p = 0.055$ ). After the ion implantation of Ca, the mean cell number at day 7 was lowest compared with the other groups, and no significant increase compared with day 1 could be calculated ( $p = 0.24$ ).

In summary, the type of production of the discs did not inhibit the adhesion and proliferation of human osteoblastic cells. All tested groups showed an increase in cell numbers over time.

In addition, by comparing all tested groups of material surfaces, no statistically significant difference was observed ( $p > 0.99$ ).

### 3.3. Optimized Centrifugal Casting Did Not Impair Osteogenic Differentiation

In the presented work, we also investigated whether osteogenic differentiation of human osteoblasts was influenced by cultivation on cast surfaces or reference material. Target genes for the analysis of osteogenic differentiation markers on gene expression levels were RUNX2, SP7, COL1a1, ALP and BGLAP, and markers for bone homeostasis were OPG, RANKL, and CASP3 for the induction of cell apoptosis, as shown in Figure 6.

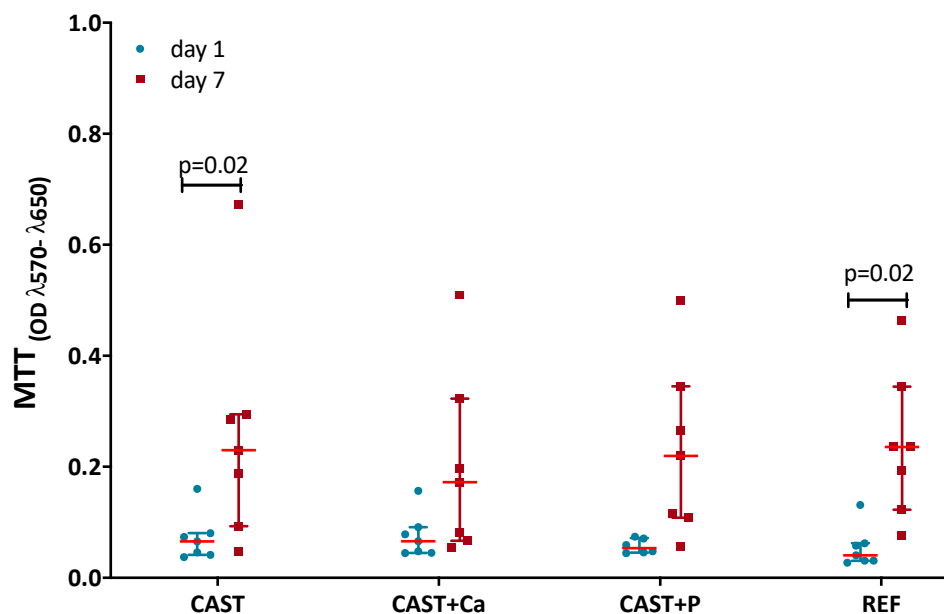


**Figure 5.** Cell proliferation tested by MTT-assay. Besides the comparison of reference material (REF) and cast specimens (CAST), the influence of beamline-implanted Ca- or P-ions into surfaces on cytotoxicity/proliferation was also tested. The proliferation of osteoblasts on the surfaces was investigated on day 1 and day 7 ( $n = 7$  each). The quotients of OD 570–650 nm were measured, and respective values are shown as scatter plots with Median and interquartile ranges. Influences of time as well as surfaces were analyzed by two-way ANOVA and Bonferroni post hoc tests for statistical significance. The significance level was set to  $p \leq 0.05$ . OD: Optical Density; Ca: Ca-ion; P: P-ion; Implantation dose  $1 \times 10^{-16} \text{ cm}^2$ , implantation energy 30 keV.

The Runt-related transcription factor 2 (RUNX2) as a key regulator of osteoblast differentiation was expressed in equal amounts on all tested surfaces. Additionally, the expression of transcription factor SP7 (Osterix), a regulator of osteogenic differentiation that enhances the effect of RUNX2, was not modulated by the different surfaces. So, the main transcriptional regulators of osteogenic differentiation were not influenced by the centrifugal cast materials.

In addition, later relevant gene expressions of the osteoblastic phenotype, like COL1a1 (collagen type I, the essential collagenous component for building bone matrix), ALP (Alkaline phosphatase, needed for mineralization of bone matrix), and BGLAP (Osteocalcin, needed to build hydroxyapatite crystals within the bone matrix), were not significantly modulated over the tested time period of 7 days.

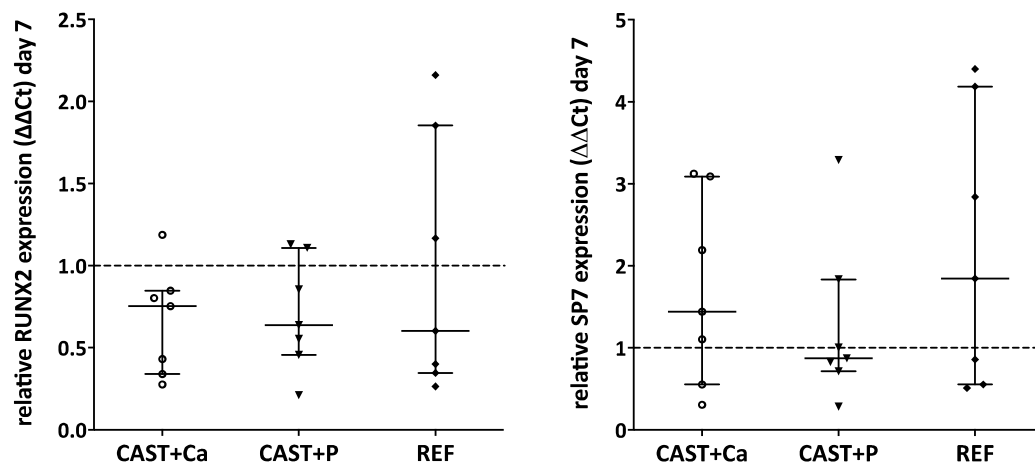
With respect to bone resorption, the tested marker genes OPG (inhibitor of bone resorption) and RANKL (stimulator of bone resorption) showed no significant differences between the CAST and reference specimen (OPG  $p = 0.22$ , RANKL  $p > 0.99$ ). However, the implantation of Ca- ( $p = 0.015$ ) or P-ions ( $p = 0.005$ ) significantly reduced the gene expression level for OPG. The expression for RANKL was not modified for any group ( $p > 0.99$ ).

The induction of apoptosis to the osteoblasts was tested by CASP3 analysis. Caspase 3 is a key regulator for cell death. No significant difference ( $p = 0.999$ ) on gene expression level was observed after 7 days of cultivation on the tested specimen.

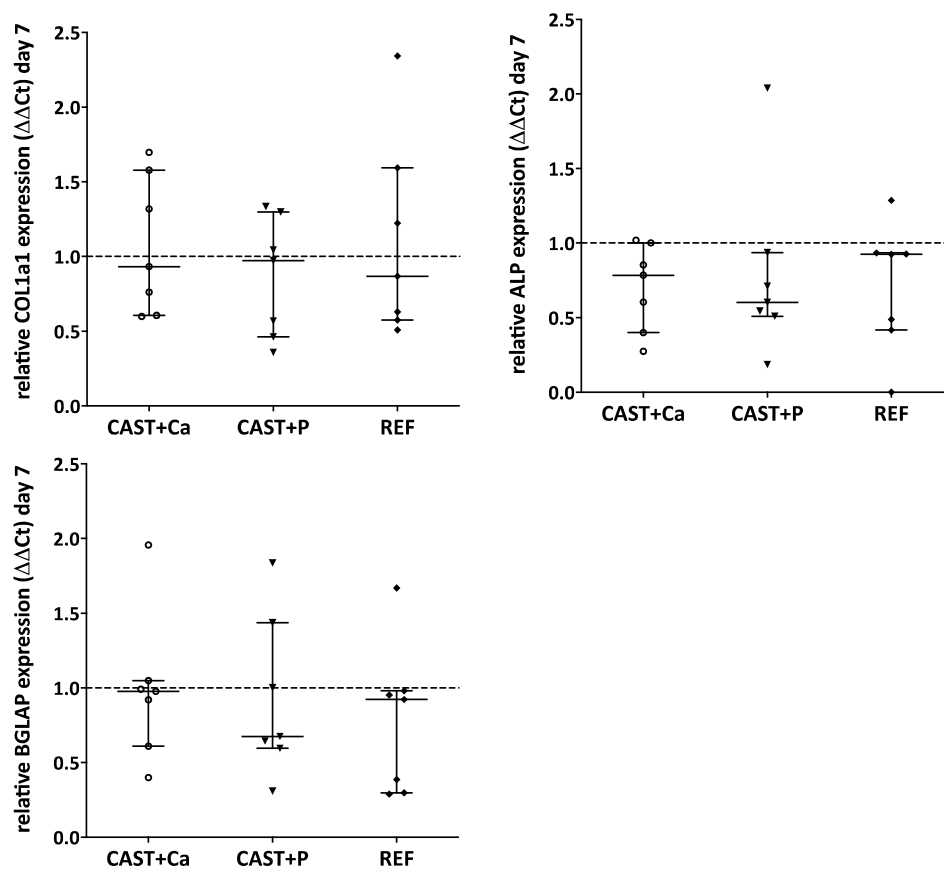
In summary, on gene expression level, the spin-cast and the reference material did not show significant differences. In terms of cast material, the additional Ca-/P-ion implantation significantly reduced the gene expression level of OPG.

We further analyzed the ongoing differentiation process of protein and on mineralization levels by quantification of C-terminal collagen type I propeptide (CICP) as a measure of collagen type I

synthesis and Osteoprotegerin (OPG), as well as Alizarin red S staining, as shown in Figure 7. All data on protein expression were normalized to the respective MTT values as a measure of cell number.

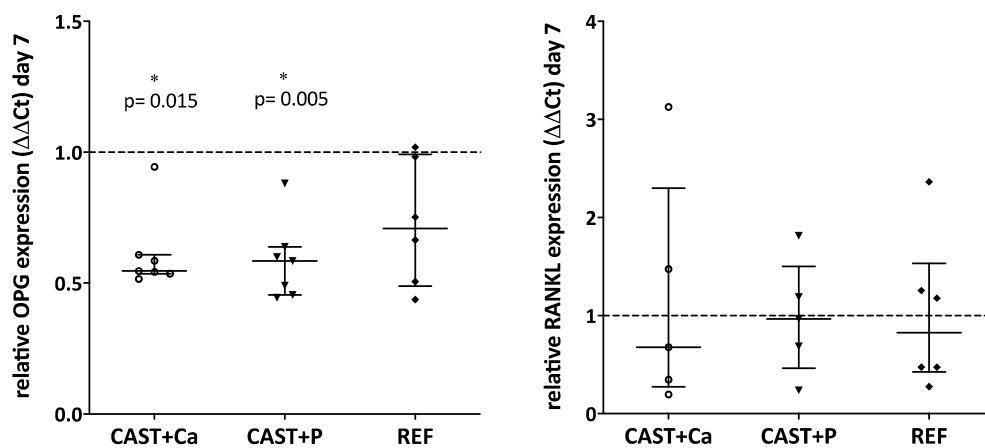


(a) Regulators of gene expression RUNX2 and SP7.

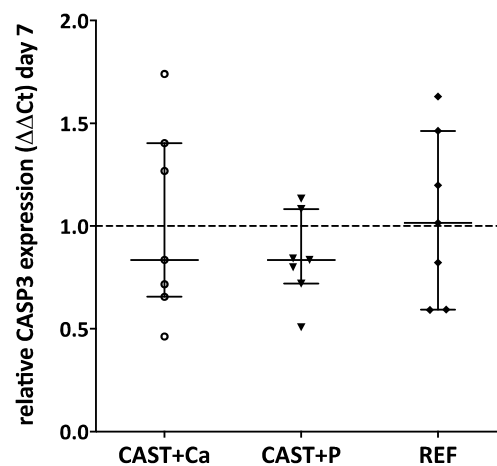


(b) Markers for differentiation COL1a1, ALP and BGLAP.

Figure 6. Cont.



(c) Marker for bone homeostasis OPG and RANKL.



(d) Marker for apoptotic process CASP3.

**Figure 6.** Gene expression analysis of primary human osteoblasts after cultivation for 7 days on a cast Ti6Al4V specimen without and with Ca- or P-ion implantation as well as a reference Ti6Al4V-specimen. Diagramed are scatterplots showing the interquartile range of the calculated  $\Delta\Delta\text{Ct}$  gene expression. (a) Shows results of regulators of the osteogenic phenotype. While RUNX2 (Runt-related transcription factor 2) is a key regulator in osteoblast differentiation, SP7 (Osterix) is a regulator of osteogenic differentiation and enhances the effect of RUNX2. (b) Presents the gene expression of differentiated osteoblasts. COL1a1: collagen type I is the major structural protein of bone. ALP: alkaline phosphatase is needed for mineralization of bone matrix and BGLAP: osteocalcin is needed to build hydroxyapatite crystals within the bone matrix. (c) Markers for bone homeostasis. OPG: osteoprotegerin is a decoy receptor for RANKL (receptor activator of nuclear factor kappa-B ligand), while RANKL normally binds to RANK in order to stimulate bone resorption by osteoclasts. (d) Marker for the apoptotic process. CASP3: caspase 3 is a predominant caspase and regulates cell apoptosis. Gene expression was normalized in osteoblasts cultivated on cast surfaces without ion implantation. All gene expression data were normalized internal to HPRT1 as a housekeeping gene. Statistical analysis by one-way ANOVA with Kruskal–Wallis and Dunn’s post hoc test. The significance level was set to  $p < 0.05$  (\*). Ca: Ca-ion; P: P-ion. Ion dose  $1 \times 10^{-16} \text{ cm}^2$ , implantation energy 30 keV;  $n = 7$ .

The CICP concentration in the cell culture supernatant, reflecting the amount of procollagen type I biosynthesis by the osteoblasts seeded on cast surfaces, declined from day 3 (730.2 pg/mL) until day 7 (272.4 pg/mL,  $p < 0.07$ ), indicating a negative feedback mechanism of pericellular collagen

type I accumulation (Figure 7a). Osteoblasts seeded on reference surfaces produced, according to the current standard method, similar results (day 3: 912 pg/mL; day 7: 240 pg/mL) for CICP-concentration, although the decline was statistically significant in this case. In the cell culture supernatant of Ca-ion implanted casting surfaces, a CICP level of 706.8 pg/mL could be observed, while on day 7 the secretion decreased 1.7-fold to 415 pg/mL ( $p > 0.99$ ). The amount of CICP in the cell culture supernatant of P-ion implanted casting surfaces was somewhat lower compared with Ca-ion implanted surfaces, although the difference was not significant. Over time, the median CICP of 611.5 pg/mL decreased by a factor of 2.5 to 244 pg/mL ( $p = 0.09$ ) on day 7. In the cell culture supernatant of the reference surfaces, a 3.8-fold significant decrease in CICP to 239.5 pg/mL was observed on day 7 ( $p = 0.005$ ). Overall, no significant difference in type I procollagen production of osteoblasts on cast surfaces without or with ion implantation could be determined compared with the reference surfaces.

OPG served as a bone turnover marker and is produced by osteoblasts to counteract bone resorption by osteoclasts. OPG is a decoy receptor for RANKL in the RANK/RANKL/OPG axis and is essential to bone metabolism. On the non-ion-implanted casting surfaces, normalized to MTT-values, an OPG release of 2673 pg/mL could be measured on day 7 (Figure 7b). Furthermore, it was shown that the OPG concentration in the cell culture supernatant of Ca-ion implanted cast surfaces was 3840 pg/mL and thus 1.4 times higher than P-ions implanted surfaces (2779 pg/mL). The OPG secretion of the osteoblasts, cultivated on reference surfaces, was similar to cast surfaces without and with P-ion implanted surfaces (median of 2833 pg/mL). Overall, there were no significant differences for OPG release of human osteoblastic cells on the surfaces ( $p < 0.99$ ).

Figure 7c presents data of an Alizarin red S staining of osteoblast-like cells cultivated on cast material and on reference material shown after 14 days. The median Alizarin red S concentration of osteoblasts on casting surfaces was 139.0  $\mu\text{g/mL}$ . For reference discs, a median Alizarin red S concentration of 152.3  $\mu\text{g/mL}$  was measured. There was no significant difference between reference and cast surfaces ( $p = 0.88$ ). The Alizarin red S values of the cells cultivated on the Ca-ion implanted surfaces was significantly reduced by 27.8% compared with non-modified cast surfaces ( $p = 0.02$ ). For P-ion implantation in casting material, the values were also somewhat lower compared with non-ion-implanted material but not significantly different ( $p = 0.16$ ). Neither comparing CAST-Ca ( $p = 0.15$ ) nor CAST-P ( $p = 0.30$ ) with the reference material showed statistically significant differences.

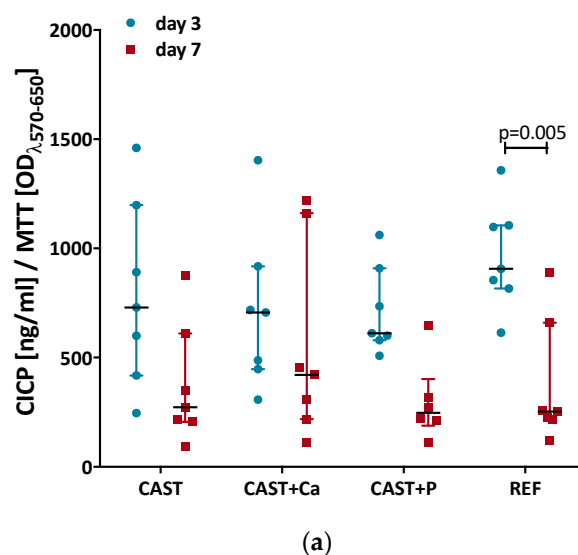
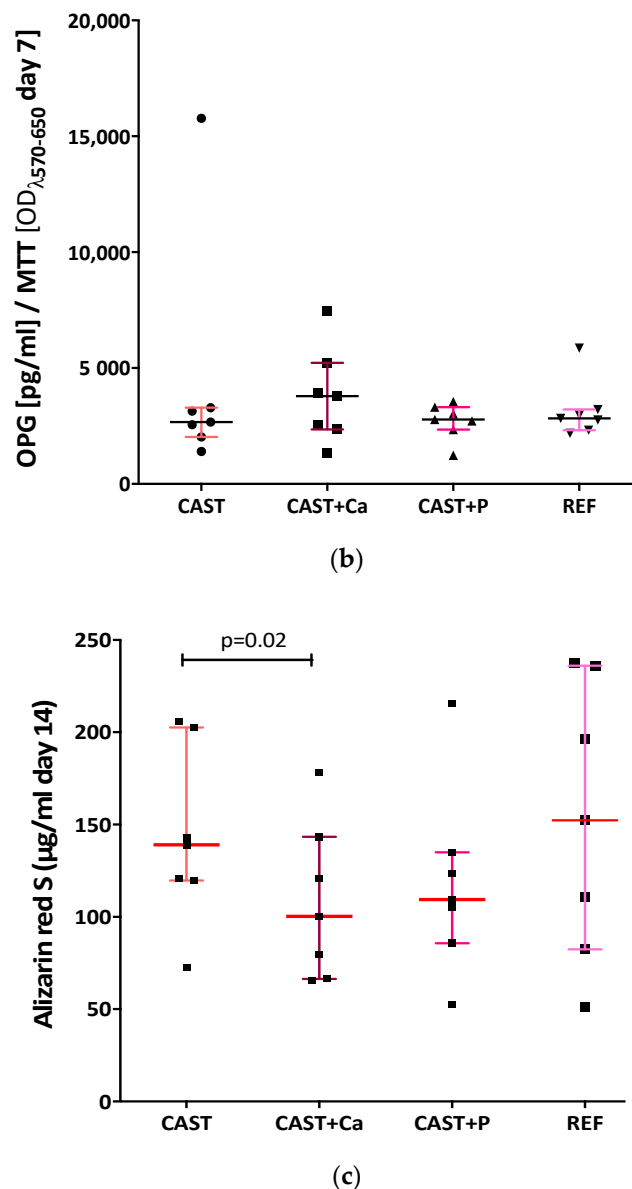


Figure 7. Cont.





**Figure 7.** Detection of in vitro mineralization and protein secretion. (a) C1CIP Elisa for collagen type I synthesis after osteoblast cultivation for 3 and 7 days. Influence of different surfaces on collagen type I synthesis was tested by a two-way ANOVA with Bonferroni post hoc test. (b) OPG Elisa results of osteoblast cultures after 7 days cultivation. Data were analyzed by using Kruskal–Wallis and Dunn’s post hoc tests for statistical significance. (c) Alizarin red S staining was used to analyze the mineralization of osteoblasts’ seeded specimens and the effect of Ca- or P-Ion coated surfaces after 14 days. Statistical analysis was done by a one-way ANOVA with a Tukey post hoc test. The significance level was set to  $p \leq 0.05$ . Values are shown as scatter plots with Median and interquartile range. Ca-ion and P-ion implantation by ion dose  $1 \times 10^{-16} \text{ cm}^2$ , implantation energy 30 keV;  $n = 7$ .

In summary, this cell biologic analyses showed that there was no significant difference between the examined cast surfaces and the reference surfaces with regard to procollagen type I and OPG secretion as well as in vitro mineralization. The additional ion implantation of Ca or P did not show any supportive effect either.

#### 4. Discussion

We aimed to show that an optimized spin casting process of Ti6Al4V, a frequently used titanium alloy for the production of hip endoprostheses for uncemented implantation, can generate material surface characteristics with comparable *in vitro* biocompatibility for primary human osteoblasts as the standard machined manufacturing process. Ion beam implantation of calcium or phosphorus following aluminum oxide blasting of the cast material, however, did not further improve the cell-biologic outcome in the dosage used.

With respect to material properties, standardized analysis did not reveal an indication of Alpha Case formation, confirming the positive effect of the optimized casting process with respect to metallurgical quality. Furthermore, chemical composition of the cast parts was within the specification. Therefore, no relevant reaction between melt and crucible or shell mold could be observed. Additionally, subsequent aluminum oxide blasting led to expected surface roughness with no significant difference to the reference machined material.

*In vivo* bone response to cast titanium implants in the tibia metaphysis has been previously studied in a rabbit and a rat model [4,19]. Mohammadi et al. used cast pure titanium from which about 0.25 mm of the superficial layer was eliminated by machining to remove impurities created by the casting process [19]. Our recent publication on a rat model was based on the same optimized casting process of the titanium alloy Ti6Al4V without removal of the superficial layer before aluminum oxide blasting, as used in the present study [4]. In both animal models, no significant difference in osseointegration after 3 months (rabbit and rat) or 6 months (rabbit) in comparison to the respective machined control implants could be observed. Recently, with respect to the treatment of large bone defects, a porous cast titanium alloy (Ti6Al7Nb) was reported to possess good *in vitro* and *in vivo* biocompatibility after acid etching [20]. We are not aware, however, of any previous *in vitro* studies on the cell-biologic response of osteogenic cells in contact with cast titanium or titanium alloy without mechanical or chemical removal of the superficial layer.

To address this knowledge gap in a clinically relevant manner, we used the established optimized casting process for Ti6Al4V, an aluminum oxide blasting process currently included in the commercial medical implant production and tested the interaction of primary human osteoblasts from patients with end-stage knee osteoarthritis who received joint-replacement surgery as a cell source. Moreover, a broad set of relevant central cell-biologic outcome parameters, such as osteoblast adhesion and proliferation, markers of early and late osteogenic differentiation, as well as secretion of signaling molecules reflecting bone turnover, was analyzed.

For both reference and cast material, we observed relatively large variation in the cell-biologic outcome parameters. This can be attributed to the use of primary human osteoblast cultures from different patients and is a common observation for non-cell lines. Nevertheless, testing primary human cells instead of using commercially available (immortalized or tumor-derived) cell-lines has been recommended in the literature [21].

Regarding cell adhesion and the proliferation of human osteoblasts on the tested specimen of spin cast or machined Ti6Al4V material, no difference was detectable. For the interpretation of these results, it is important that the process of aluminum oxide blasting resulted in nearly identical surface roughness. That the microstructure of the surface represents an essential factor for cell adhesion, proliferation and differentiation is well known and has been the subject of comprehensive reviews, for example by Mitra et al. [22]. Yokose and co-worker demonstrated that the surface micro topography of titanium discs influences osteoblast-like cell proliferation and differentiation [23]. Moreover, Hatano et al. reported that primary rat osteoblasts showed higher proliferation, and alkaline phosphatase and osteocalcin expression cultivated on rough rather than smooth tissue culture polystyrene [24]. It is also known from the literature that roughness of the surface is important for a successful osseointegration [25]. In addition to classical micro and nano topography, the presence of pores within the surface also has a major influence on cell adhesion and differentiation of the desired cells [22]. Thus, further improvement of integration can be achieved, for example, by using multi scale porous titanium

surfaces rather than smooth or micro-roughened titanium [25]. According to results from Anselme and coworkers, our findings indicate a similar biocompatibility of the reference and cast material since the surface topography, generated by classical aluminum-oxide blasting, was not different [26,27]. As previously reported by Lagonegro et al., we observed that human osteoblasts preferentially adhered to the peaks of micro-topography and bridged over geometric surface irregularities [23,28].

A similar observation was published by Yin et al. [29]. The authors showed that the blasting or etching of a titanium surface has a significant effect on osteoblast differentiation. Rough-blasted surfaces supported the differentiation process while the etching process reduced the expression of osteoblast markers like RUNX2, COL1a1, and ALP. We also tested these osteogenic differentiation markers on human primary osteoblasts and found no significant difference between the reference machined material and the cast specimen. The same result was obtained for the expression of BGLAP as a late marker of osteoblast phenotype and the *in vitro* mineralization determined by Alizarin Red Assay. These findings are in line with the recently published results of Wölfle-Roos et al. [4]. They showed that in rats *in vivo* no negative effect with respect to bone-implant contact or pull-out-force could be attributed to the optimized manufacturing process, which was also used in the present *in vitro* experiments.

Some titanium surfaces in the *in vitro* study were further modified by ion beam implantation of Ca- or P-ions. Comparing our data with the available literature on similar surface modifications, some divergences need to be discussed. Krupa et al. presented similar results for human bone derived cells when seeded on mirror polished pure commercial Ti-surfaces. They used similar conditions for ion implantation and found no adverse biological effects in terms of cell viability and ALP analysis [30,31]. In addition, Nayab et al. could not detect any effect on MG63 cells after seeding on pure Ti-surfaces with implanted Ca ions (ion dose  $1 \times 10^{-15}$  or  $1 \times 10^{-16}$ ). Only by using higher concentrations of Ca (ion dose  $1 \times 10^{-17}$ ) did they describe slightly better cell spreading, associated with delayed adhesion and enhanced expression of bone cell markers [32,33]. Several working groups could demonstrate a positive effect on cellular behavior by coating titanium surfaces with calcium or phosphor [34–37]. Besides the different metallic materials, pure titanium vs. Ti6Al4V, they also used different techniques for surface modification like plasma spraying or chemical methods. Therefore, the amount of biologically available ions is not comparable [33]. By using ion implantation, the ions become dispersed into a certain range of depth and a relevant part of them becomes not bioavailable [13]. Thus, besides ion density, implantation energy also influences biological impact. Moreover, the vast majority of *in vitro* studies are not based on sand-blasted or etched surfaces with a roughness comparable to the current clinical application. In the case of a relevant surface micro-roughness plasma, ion implantation of calcium, used in the study of Cheng et al., could also have advantages [38]. The authors found significant positive effects of calcium plasma immersion ion implantation on the osteoblast-like cell line MG63 with respect to adhesion, proliferation and osteogenic differentiation *in vitro* and in a rabbit *in vivo* model. However, besides the different ion implantation technique and dosage, the use of pure machined titanium, a lower degree of surface micro-roughness and the analysis of a bone-tumor derived cell-line instead of primary human osteoblasts in this study precludes a direct comparison. The encouraging results nevertheless indicate that different strategies and dosages of ion implantation should be further studied with our optimized spin cast Ti6Al4V-alloy.

Additionally, the charge of the surface modulates cellular activities. In our study, the addition of Ca- or P-ions by ion beam implantation even negatively affected mineral deposition in the synthesized collagen matrix, as shown by Alizarin red S staining. This is somewhat contrary to the so far known literature [36,39]. One explanation could be the fact that these groups used different methods for surface modifications than we did. They used chemical approaches or, like Knabe et al., plasma spraying to cover the titanium with Ca- or Zn-P-ions [35]. It could be possible that the surface charge was not changed in an analogous manner in addition to a different amount of deposition and the bioavailability of the ions when using these alternative surface modification techniques. In future experiments, a similar approach to investigating surface charge changes as described by Kulkarni

and co-workers could be used [40]. They presented data on how surface characteristics influence interaction with small sized model proteins. Namely, variations in charge densities towards the top edges of the surface seem to be a relevant factor. This effect was shown to be mainly triggered by nano topography [41]. Due the identical production process of our cast specimen and the not significantly different results of Ra and Rz without/with ion implantation, we conclude that any possible differences in the charge density in the case of ion implantation could be due to the deposition itself or to influences on the nanostructure, which was not analyzed in this study. Future experiments should consider studying nano-topographic features and analysis of wettability as well as zeta potential.

In terms of cell apoptosis, we tested for the gene expression of CASP3, a key member of the apoptotic pathway in osteogenic cells undergoing differentiation [42]. Even using the same alloy for reference and cast specimens, treating them in the same medical grade production process, including aluminum oxide blasting and sterilization procedures with the same machinery, it could have been possible that different micro- or nano-topographic structures could have led to unwanted cell death of the osteoblasts. This relevant topic has been disused by several groups. Kulkarni et al. showed that the titanium alloy surface topography influences cell survival and cell death [43]. Unfortunately, the rough micro-topography of the specimen did not allow for a reliable measurement of the nano-topography that could somehow be different in the machined references and the cast specimen. Besides that, some knowledge arises that cytotoxic effects of Titanium and its alloys have to be considered [44]. Nevertheless, Ti6Al4V is the most frequently and successfully used alloy in orthopedic surgery because of its biocompatibility and certain bone-similar characteristics. Therefore, the present work focused on the transfer of the routine fabrication of this alloy to a newly developed fabrication method.

It was also reported that, besides the overexpression of CASP3, which leads to unwanted cell death, a loss of CASP3 expression results in delayed ossification and decreased bone mineral density. Comparing our reference material with that of the cast, we could conclude that the given CASP3 expression does not impair the osteogenic differentiation process and preserves the viability of osteoblasts. Also, our data indicate no respective difference in CASP3 expression between the tested specimens.

Because of the non-loaded in vitro conditions, a possible impact on inflammatory processes should be further tested by including, for example, abrasion experiments and by studying interaction with macrophages. Under unloaded in vitro conditions, the analysis of osteoblast OPG and RANKL expression on the gene and protein level did not indicate any disadvantage of the optimized casting process in terms of secretion of central regulators of osteoclast activity in the present study. These results are in line with our data from the in vivo study in which no relevant induction of inflammation or subsequent bone resorption or local osteolysis was observed after the implantation of small rods in the tibia metaphysis of rats [4]. Nevertheless, it should be kept in mind that further testing in a load-bearing large animal model still has to be performed.

The optimized casting process was successfully developed in terms of methods and practical procedure and is currently the subject of further research, aiming to create a scalable production process for market-ready implants. So far, produced tibia and femur prototypes meet given demands regarding microstructure as well as mechanical and machining properties. Approaching industrial part production, the process is now in the development stage to facilitate upscaled production lots for the fabrication of uncemented endoprostheses at competitive market prices. Besides the still-required increase in productivity, the improvement of dimensional accuracy is being addressed as a secondary challenge as methods to correct it are successfully employed regularly. Finally, in addition to comparison with standard machined Ti6Al4V, material comparative testing of spin cast Ti6Al4V with other Titanium alloys, like Ti6Al7Nb or Ti28Nb35.4Zr, should be performed.

## 5. Conclusions

It can be stated that the surfaces produced in the optimized casting process of Ti6Al4V are not different from the reference surfaces of the same alloy successfully used in orthopedic surgery with

respect to cell-biologic interactions of human osteoblasts in vitro. Neither a difference in cell spreading, cell viability/proliferation nor an influence on osteogenic differentiation and mineralization of primary osteoblasts was detectable. The optimized casting process, therefore, provided equivalent biologic material quality in this first comprehensive in vitro analysis based on primary human osteoblasts. These results confirm our recent in vivo data on osseointegration in a rat model. [4] Thus, near net-shape precision casting of Ti6Al4V, avoiding high demand of stock material for machining as well as the cost for the machining itself, may present a promising and cost-effective alternative to the conventional machining-based process for uncemented orthopedic implants.

Ion implantation of calcium or phosphorus by ion beam, however, did not induce a positive effect on human osteoblastic cells in vitro, again confirming our previous data on osseointegration in the rat model [4] despite the use of different ion-implantation techniques (ion-beam versus plasma ion implantation), which makes the results not directly comparable. Therefore, further studies on the effect of different ion implantation doses should be performed.

**Author Contributions:** Conceptualization, B.R.E., F.J., M.H., K.G. and K.A.B.; methodology, B.R.E., F.J., M.H., K.G. and K.A.B.; validation, B.R.E., F.J., M.H., K.G. and K.A.B.; formal analysis, K.A.B., M.H. and K.G.; investigation, K.A.B., M.H. and K.G.; resources, B.R.E., M.H. and K.G.; data curation, F.J., M.H. and K.G.; writing—original draft preparation, J.F.; writing—review and editing, F.J., B.R.E., M.H., K.A.B. and K.G.; visualization, F.J. and M.H.; supervision, B.R.E.; project administration, B.R.E., M.H., K.G. and K.A.B.; funding acquisition, B.R.E. All authors have read and agreed to the published version of the manuscript.

**Funding:** This study has been funded by a grant from the German Federal Ministry of Education and Research (BMBF, No. 13 GW0020B/E).

**Acknowledgments:** We wish to acknowledge the support of Giovanni Ravalli for technical assistance and Paul Walther (Department of electron microscopy, University of Ulm, Germany) for his support in the electron microscopic studies). We gratefully thank Andreas Kolitsch from the Helmholtz-Zentrum Dresden-Rossendorf (HZDR) for the ion beam implantation.

**Conflicts of Interest:** The funders had no role in the design of the study; in the collection, analyses, or interpretation of data; in the writing of the manuscript, or in the decision to publish the results. The authors declare no conflict of interest.

## References

1. Ha, S.-W.; Wintermantel, E. Biokompatible Metalle. In *Medizintechnik*, 5th ed.; Wintermantel, E., Ha, S., Eds.; Springer: Berlin/Heidelberg, Germany, 2009; pp. 191–217. [\[CrossRef\]](#)
2. Nastac, L.; Gungor, M.N.; Ucok, I.; Klug, K.L.; Tack, W.T. Advances in investment casting of Ti–6Al–4V alloy: A review. *Int. J. Cast Met. Res.* **2013**, *19*, 73–93. [\[CrossRef\]](#)
3. Billhofer, H.; Hauptmann, T. Feingussystem für Titan und Titanlegierungen. *Lightweight Des.* **2010**, *3*, 47–51. [\[CrossRef\]](#)
4. Wolfle-Roos, J.V.; Katmer Amet, B.; Fiedler, J.; Michels, H.; Kappelt, G.; Ignatius, A.; Durselen, L.; Reichel, H.; Brenner, R.E. Optimizing Manufacturing and Osseointegration of Ti6Al4V Implants through Precision Casting and Calcium and Phosphorus Ion Implantation? In Vivo Results of a Large-Scale Animal Trial. *Materials* **2020**, *13*, 1670. [\[CrossRef\]](#)
5. Kienapfel, H.; Sprey, C.; Wilke, A.; Griss, P. Implant fixation by bone ingrowth. *J. Arthroplast.* **1999**, *14*, 355–368. [\[CrossRef\]](#)
6. Wolfle, J.V.; Fiedler, J.; Durselen, L.; Reichert, J.; Scharnweber, D.; Forster, A.; Schwenzer, B.; Reichel, H.; Ignatius, A.; Brenner, R.E. Improved anchorage of Ti6Al4V orthopaedic bone implants through oligonucleotide mediated immobilization of BMP-2 in osteoporotic rats. *PLoS ONE* **2014**, *9*, e86151. [\[CrossRef\]](#)
7. Krupa, D.; Baszkiewicz, J.; Kozubowski, J.A.; Barcz, A.; Sobczak, J.W.; Bilinski, A.; Lewandowska-Szumiel, M.; Rajchel, B. Effect of dual ion implantation of calcium and phosphorus on the properties of titanium. *Biomaterials* **2005**, *26*, 2847–2856. [\[CrossRef\]](#)
8. Lazarinis, S.; Makela, K.T.; Eskelinen, A.; Havelin, L.; Hallan, G.; Overgaard, S.; Pedersen, A.B.; Karrholm, J.; Hailer, N.P. Does hydroxyapatite coating of uncemented cups improve long-term survival? An analysis of 28,605 primary total hip arthroplasty procedures from the Nordic Arthroplasty Register Association (NARA). *Osteoarthr. Cartil.* **2017**, *25*, 1980–1987. [\[CrossRef\]](#)



9. Surmenev, R.A.; Surmeneva, M.A.; Ivanova, A.A. Significance of calcium phosphate coatings for the enhancement of new bone osteogenesis—A review. *Acta Biomater.* **2014**, *10*, 557–579. [[CrossRef](#)]
10. Pham, M.T.; Reuther, H.; Matz, W.; Mueller, R.; Steiner, G.; Oswald, S.; Zyganov, I. Surface induced reactivity for titanium by ion implantation. *J. Mater. Sci. Mater. Med.* **2000**, *11*, 383–391. [[CrossRef](#)]
11. Rautray, T.R.; Narayanan, R.; Kwon, T.Y.; Kim, K.H. Surface modification of titanium and titanium alloys by ion implantation. *J. Biomed. Mater. Res. B Appl. Biomater.* **2010**, *93*, 581–591. [[CrossRef](#)]
12. Biggs, M.J.; Richards, R.G.; Gadegaard, N.; Wilkinson, C.D.; Dalby, M.J. The effects of nanoscale pits on primary human osteoblast adhesion formation and cellular spreading. *J. Mater. Sci. Mater. Med.* **2007**, *18*, 399–404. [[CrossRef](#)] [[PubMed](#)]
13. Dalby, M.J.; Yarwood, S.J.; Riehle, M.O.; Johnstone, H.J.; Affrossman, S.; Curtis, A.S. Increasing fibroblast response to materials using nanotopography: Morphological and genetic measurements of cell response to 13-nm-high polymer demixed islands. *Exp. Cell Res.* **2002**, *276*, 1–9. [[CrossRef](#)] [[PubMed](#)]
14. Kiang, J.D.; Wen, J.H.; del Alamo, J.C.; Engler, A.J. Dynamic and reversible surface topography influences cell morphology. *J. Biomed. Mater. Res. A* **2013**, *101*, 2313–2321. [[CrossRef](#)]
15. Fiedler, J.; Kolitsch, A.; Kleffner, B.; Henke, D.; Stenger, S.; Brenner, R.E. Copper and silver ion implantation of aluminium oxide-blasted titanium surfaces: Proliferative response of osteoblasts and antibacterial effects. *Int. J. Artif. Organs* **2011**, *34*, 882–888. [[CrossRef](#)] [[PubMed](#)]
16. Fiedler, J.; Ozdemir, B.; Bartholoma, J.; Plettl, A.; Brenner, R.E.; Ziemann, P. The effect of substrate surface nanotopography on the behavior of multipotent mesenchymal stromal cells and osteoblasts. *Biomaterials* **2013**, *34*, 8851–8859. [[CrossRef](#)]
17. Mane, V.P.; Heuer, M.A.; Hillyer, P.; Navarro, M.B.; Rabin, R.L. Systematic method for determining an ideal housekeeping gene for real-time PCR analysis. *J. Biomol. Tech.* **2008**, *19*, 342–347.
18. Katmer Amet, B. Bewertung von Ti-6Al-4V Oberflächen Hergestellt Mittels neu Entwickelter Schleudergusstechnologie im In Vitro- und In Vivo-Modell. Ph.D. Thesis, University of Ulm, Ulm, Germany, 2019. [[CrossRef](#)]
19. Mohammadi, S.; Esposito, M.; Wictorin, L.; Aronsson, B.O.; Thomsen, P. Bone response to machined cast titanium implants. *J. Mater. Sci.* **2001**, *36*, 1987–1993. [[CrossRef](#)]
20. Sommer, U.; Laurich, S.; de Azevedo, L.; Viehoff, K.; Wenisch, S.; Thormann, U.; Alt, V.; Heiss, C.; Schnettler, R. In Vitro and In Vivo Biocompatibility Studies of a Cast and Coated Titanium Alloy. *Molecules* **2020**, *25*, 3399. [[CrossRef](#)]
21. Czekanska, E.M.; Stoddart, M.J.; Ralphs, J.R.; Richards, R.G.; Hayes, J.S. A phenotypic comparison of osteoblast cell lines versus human primary osteoblasts for biomaterials testing. *J. Biomed. Mater. Res. A* **2014**, *102*, 2636–2643. [[CrossRef](#)]
22. Mitra, J.; Tripathi, G.; Sharma, A.; Basu, B. Scaffolds for bone tissue engineering: Role of surface patterning on osteoblast response. *RSC Adv.* **2013**, *3*, 11073–11094. [[CrossRef](#)]
23. Yokose, S.; Klokkevold, P.R.; Takei, H.H.; Kadokura, H.; Kikui, T.; Hibino, Y.; Shigeta, H.; Nakajima, H.; Kawazu, H. Effects of surface microtopography of titanium disks on cell proliferation and differentiation of osteoblast-like cells isolated from rat calvariae. *Dent. Mater. J.* **2018**, *37*, 272–277. [[CrossRef](#)] [[PubMed](#)]
24. Hatano, K.; Inoue, H.; Kojo, T.; Matsunaga, T.; Tsujisawa, T.; Uchiyama, C.; Uchida, Y. Effect of surface roughness on proliferation and alkaline phosphatase expression of rat calvarial cells cultured on polystyrene. *Bone* **1999**, *25*, 439–445. [[CrossRef](#)]
25. Jang, T.S.; Jung, H.D.; Kim, S.; Moon, B.S.; Baek, J.; Park, C.; Song, J.; Kim, H.E. Multiscale porous titanium surfaces via a two-step etching process for improved mechanical and biological performance. *Biomed. Mater.* **2017**, *12*, 025008. [[CrossRef](#)] [[PubMed](#)]
26. Anselme, K. Osteoblast adhesion on biomaterials. *Biomaterials* **2000**, *21*, 667–681. [[CrossRef](#)]
27. Anselme, K.; Noel, B.; Hardouin, P. Human osteoblast adhesion on titanium alloy, stainless steel, glass and plastic substrates with same surface topography. *J. Mater. Sci. Mater. Med.* **1999**, *10*, 815–819. [[CrossRef](#)]
28. Lagonegro, P.; Trevisi, G.; Nasi, L.; Parisi, L.; Manfredi, E.; Lumetti, S.; Rossi, F.; Macaluso, G.M.; Salviati, G.; Galli, C. Osteoblasts preferentially adhere to peaks on micro-structured titanium. *Dent. Mater. J.* **2018**, *37*, 278–285. [[CrossRef](#)]
29. Yin, C.; Zhang, Y.; Cai, Q.; Li, B.; Yang, H.; Wang, H.; Qi, H.; Zhou, Y.; Meng, W. Effects of the micro-nano surface topography of titanium alloy on the biological responses of osteoblast. *J. Biomed. Mater. Res. A* **2017**, *105*, 757–769. [[CrossRef](#)]

30. Krupa, D.; Baszkiewicz, J.; Kozubowski, J.A.; Barcz, A.; Sobczak, J.W.; Bilinski, A.; Lewandowska-Szumiel, M.D.; Rajchel, B. Effect of calcium-ion implantation on the corrosion resistance and biocompatibility of titanium. *Biomaterials* **2001**, *22*, 2139–2151. [\[CrossRef\]](#)
31. Krupa, D.; Baszkiewicz, J.; Kozubowski, J.A.; Barcz, A.; Sobczak, J.W.; Bilinski, A.; Lewandowska-Szumiel, M.; Rajchel, B. Effect of phosphorus-ion implantation on the corrosion resistance and biocompatibility of titanium. *Biomaterials* **2002**, *23*, 3329–3340. [\[CrossRef\]](#)
32. Nayab, S.N.; Jones, F.H.; Olsen, I. Effects of calcium ion implantation on human bone cell interaction with titanium. *Biomaterials* **2005**, *26*, 4717–4727. [\[CrossRef\]](#)
33. Nayab, S.N.; Jones, F.H.; Olsen, I. Effects of calcium ion-implantation of titanium on bone cell function in vitro. *J. Biomed. Mater. Res. A* **2007**, *83*, 296–302. [\[CrossRef\]](#) [\[PubMed\]](#)
34. Hotchkiss, K.M.; Reddy, G.B.; Hyzy, S.L.; Schwartz, Z.; Boyan, B.D.; Olivares-Navarrete, R. Titanium surface characteristics, including topography and wettability, alter macrophage activation. *Acta Biomater.* **2016**, *31*, 425–434. [\[CrossRef\]](#) [\[PubMed\]](#)
35. Knabe, C.; Berger, G.; Gildenhaar, R.; Klar, F.; Zreiqat, H. The modulation of osteogenesis in vitro by calcium titanium phosphate coatings. *Biomaterials* **2004**, *25*, 4911–4919. [\[CrossRef\]](#) [\[PubMed\]](#)
36. Kwon, Y.S.; Park, J.W. Osteogenic differentiation of mesenchymal stem cells modulated by a chemically modified super-hydrophilic titanium implant surface. *J. Biomater. Appl.* **2018**, *33*, 205–215. [\[CrossRef\]](#)
37. Vilardell, A.M.; Cinca, N.; Garcia-Giralt, N.; Dosta, S.; Cano, I.G.; Nogues, X.; Guilemany, J.M. Osteoblastic cell response on high-rough titanium coatings by cold spray. *J. Mater. Sci. Mater. Med.* **2018**, *29*, 19. [\[CrossRef\]](#)
38. Cheng, M.; Qiao, Y.; Wang, Q.; Jin, G.; Qin, H.; Zhao, Y.; Peng, X.; Zhang, X.; Liu, X. Calcium Plasma Implanted Titanium Surface with Hierarchical Microstructure for Improving the Bone Formation. *ACS Appl. Mater. Interfaces* **2015**, *7*, 13053–13061. [\[CrossRef\]](#)
39. Park, J.W.; Hanawa, T.; Chung, J.H. The relative effects of Ca and Mg ions on MSC osteogenesis in the surface modification of microrough Ti implants. *Int. J. Nanomed.* **2019**, *14*, 5697–5711. [\[CrossRef\]](#)
40. Kulkarni, M.; Mazare, A.; Park, J.; Gongadze, E.; Killian, M.S.; Kralj, S.; von der Mark, K.; Iglic, A.; Schmuki, P. Protein interactions with layers of TiO<sub>2</sub> nanotube and nanopore arrays: Morphology and surface charge influence. *Acta Biomater.* **2016**, *45*, 357–366. [\[CrossRef\]](#)
41. Gongadze, E.; Kabaso, D.; Bauer, S.; Slivnik, T.; Schmuki, P.; van Rienen, U.; Iglic, A. Adhesion of osteoblasts to a nanorough titanium implant surface. *Int. J. Nanomed.* **2011**, *6*, 1801–1816. [\[CrossRef\]](#)
42. Miura, M.; Chen, X.D.; Allen, M.R.; Bi, Y.; Gronthos, S.; Seo, B.M.; Lakhani, S.; Flavell, R.A.; Feng, X.H.; Robey, P.G.; et al. A crucial role of caspase-3 in osteogenic differentiation of bone marrow stromal stem cells. *J. Clin. Investig.* **2004**, *114*, 1704–1713. [\[CrossRef\]](#)
43. Kulkarni, M.; Mazare, A.; Gongadze, E.; Perutkova, Š.; Kralj-Iglič, V.; Milošev, I.; Schmuki, P.; Iglič, A.; Mozetič, M. Titanium nanostructures for biomedical applications. *Nanotechnology* **2015**, *26*, 062002. [\[CrossRef\]](#) [\[PubMed\]](#)
44. Kim, K.T.; Eo, M.Y.; Nguyen, T.T.H.; Kim, S.M. General review of titanium toxicity. *Int. J. Implant Dent.* **2019**, *5*, 10. [\[CrossRef\]](#) [\[PubMed\]](#)

**Publisher’s Note:** MDPI stays neutral with regard to jurisdictional claims in published maps and institutional affiliations.



© 2020 by the authors. Licensee MDPI, Basel, Switzerland. This article is an open access article distributed under the terms and conditions of the Creative Commons Attribution (CC BY) license (<http://creativecommons.org/licenses/by/4.0/>).